CLM-P 131

CLM-P 131

This document is intended for publication in a journal, and is made available on the understanding that extracts or references will not be published prior to publication of the original, without the consent of the authors.

United Kingdom Atomic Energy Authority

RESEARCH GROUP

Preprint

A MEASUREMEMT OF THE CROSS-SECTION FOR DETACHMENT OF ELECTRONS FROM H^- BY ELECTRON IMPACT

D. F. DANCE
M. F. A. HARRISON
R. D. RUNDEL

Culham Laboratory
Abingdon Berkshire

1967

UNCLASSIFIED
(Approved for publication)

CLM - P 131

A MEASUREMENT OF THE CROSS-SECTION FOR DETACHMENT OF ELECTRONS FROM H^- BY ELECTRON IMPACT

by

D.F. DANCE
M.F.A. HARRISON
R.D. RUNDEL

A B S T R A C T

A crossed beam method has been used to measure the cross-section for the production of neutral particles in single collisions of electrons with H^- ions at incident electron energies from 9 eV to 500 eV. The measured cross-section reaches a maximum of 50×10^{-16} cm^2 at an energy of 14 eV, and may be represented by the function

$$Q = \left(1 - \frac{1.6}{\sqrt{E \log E}}\right) \frac{950}{E} \log \frac{E}{0.92} ,$$

where the cross-section Q is in units of 10^{-16} cm^2 and the incident electron energy E in units of eV. The magnitude and functional dependence of the cross-section agree well with theoretical calculations using the Bethe-Born approximation at energies above 20 eV.

UKAEA Research Group,
Culham Laboratory,
Abingdon,
Berks.

January, 1967 (ED)

CONTENTS

1. INTRODUCTION

The reaction in which an electron is detached from the negative hydrogen ion by electron impact is an important one for several reasons. H^- is believed to contribute strongly to the opacity of stellar photospheres (Pagel, 1956, 1959). Since detachment by electron impact may be a significant mechanism for the destruction of H^-, it is necessary to know the cross-section for this reaction in order to predict whether or not the photospheric concentration of H^- is in local thermodynamic equilibrium. Electron-negative ion detachment cross-sections are also of interest in the investigation of the properties of arc plasmas (Boldt, 1959).

This reaction is most interesting, however, because there is a repulsive Coulomb force between the incident and target particles. This repulsive Coulomb force may have a strong effect upon the cross-section, especially in the region near threshold, although quantitatively its effect is not well-understood.

Theoretical calculations of the cross-section for detachment in $e-H^-$ collisions are in wide disagreement with each other. In fact, the cross-section has tended to become smaller with each new calculation that has appeared. Pagel (1956) used the classical Thomson cross-section, without Coulomb correction, which gives a cross-section whose peak value is well in excess of $1000\,\pi a_0^2$. Geltman (1960) used the Born-Oppenheimer approximation, with a semi-classical Coulomb correction to obtain a cross-section of about $700\,\pi a_0^2$ at maximum; it has since been shown, however, that Geltman's calculation is in error because the wave functions used were not orthogonal. McDowell and Williamson (1963) used the Bethe-Born approximation in conjunction with the photo-detachment calculations of John (1960) and Geltman (1962) and the Coulomb correction of Geltman (1960) to obtain a cross-section of about $70\,\pi a_0^2$ at maximum. Rudge (1964) has made a similar but more elaborate calculation. Instead of using the semi-classical Geltman Coulomb correction, he has explicitly allowed for Coulomb repulsion between the outgoing electrons in the final state of the reaction; this gives a cross-section very different in shape to those previously calculated, and with a peak value of $3.4\,\pi a_0^2$. The cross-section calculated by Smirnov and Chibisov (1966) is, at low energies, the cross-section for detachment by the Coulomb electric field, and, at high energies, the cross-section obtained from an impact parameter Bethe-Born model with a semi-classical Coulomb correction similar to Geltman's. These two cross-sections seem to have been empirically fitted together at intermediate energies to give a "total" cross section whose peak value (which lies in this intermediate energy range) is about $75\,\pi a_0^2$. Rogalski (1966) has made a Born-Oppenheimer approximation calculation, obtaining a maximum cross-section of $1400\,\pi a_0^2$.

The only experimental work on electron-negative ion collisions is that of Tisone and Branscomb (1966). They measured the detachment cross-section for $e+H^-$ over the energy range from 30 to 500 eV. Their results show general agreement with the calculations of McDowell and Williamson (1963); however, the possible errors in their experiment are large, and it can be regarded only as a semi-quantitative measurement. Furthermore, no measurements were made in the interesting energy region of one Rydberg and below, where the Coulomb correction is expected to be particularly large.

2. THE EXPERIMENT

In the present experiment, a crossed beam method was used to measure the cross-section for the reaction

$$e + H^- \rightarrow H + 2e$$

where the product H atom may be excited. A target beam of H^- was bombarded at right angles with an electron beam of variable energy, and neutral particles resulting from electron-ion collisions were detected.

The cross-section in terms of the experimental parameters is given by the expression

$$Q(E) = \frac{R}{IJ} \frac{v\,V}{(v^2 + V^2)^{\frac{1}{2}}} e^2 hF \frac{1}{\Omega} \qquad \ldots (1)$$

(Dance, Harrison, and Smith, 1966; Harrison, 1966a; Harrison, 1966b). In this equation E is the true incident electron energy given by $E = \frac{1}{2}m_e(v^2 + V^2)$, R is the signal count rate, I and J are the ion and electron beam currents, v and V are the electron and ion beam velocities, e is the electronic charge, h is the ion beam height in the collision region, Ω is the efficiency of the neutral particle detection system, and F is a beam overlap factor which takes into account inhomogeneities in the vertical current density distribution of each beam.

All of these quantities can be accurately measured and the cross-section determined absolutely.

3. APPARATUS

A schematic view of the experimental apparatus is shown in Fig.1. Except for the neutral particle detection system, the apparatus is similar to that described by Dolder, Harrison and Thonemann (1961). A mass-analysed beam of H^-, with an energy of 15 keV, is collimated by a pair of apertures 0.26 cm high by 0.10 cm wide. It then traverses a magnetically shielded collision region where it is intersected at right angles by an electron beam of variable energy. A view of the apparatus through the electron beam is shown in Fig.2. A slotted shutter can be scanned through the beams in this region in order to measure their height and vertical current density distribution. Upon leaving the collision region, the parent ion beam is separated from neutral particles by the field of the beam separator magnet and collected in a Faraday cup. Neutral particles are undeflected by this field and pass directly into the neutral product detector.

The neutral product detector and associated electronics is shown in Fig.3. This detector is moveable and for calibration purposes (Section 5) can be set in either of two positions. In one of the positions particles enter a carefully insulated and suppressed Faraday cup, and the current to this cup may be measured with a vibrating reed electrometer. In the other position, particles strike the first dynode of a 17 stage copper-beryllium venetian-blind type particle multiplier (EMI type 9643), operated as a single particle counting device. The output pulses from the multiplier are amplified, passed through a discriminator to eliminate small pulses resulting from electronic noise in the amplifiers, and counted. In either position of the detector assembly, the entrance aperture is 4 cm in height and its width is variable from 0 to 2 cm. This facility is used to ensure that the detector is large enough to collect all the beam of neutral particles.

The pressure in the collision region was typically 2×10^{-9} torr, and in the detector region 4×10^{-9} torr. The ion beam was typically 8×10^{-11}A, and the maximum usable electron current varied from 30 μA at the lowest energy to 3 mA at the highest energy.

4. BACKGROUND EFFECTS

In this experiment both the electron and ion beams were found to produce backgrounds. The total count rate was usually about 1000 per second, of which only 10 to 30 per second were true signal counts. It was ascertained that these backgrounds were not due to charged particles by placing a strong electric field near the entrance of the neutral product detector, and observing that the total count rate did not change. The electron background was probably due to bremsstrahlung photons produced by electrons striking surfaces; this background was less than 10% of the total count rate except at the highest electron energies used, where it became comparable with the ion beam background. The ion beam background was due mainly to neutral particles formed by electron detachment in collisions with residual gas, but some contribution may also have come from neutral particles or photons produced by ions striking slit edges. At the beginning of the experiment a large background was observed due to photons, which were produced in or near the ion source, being reflected by a surface in the region of the beam selector magnet and entering the neutral product detector. This background, however, was eliminated by shielding the surface to prevent reflection.

The true signal count rate was separated from the background count rates by using the double beam pulsing system described by Dance, Harrison and Smith (1966) and by Harrison (1966b). In this system (shown in Fig.4) both beams are pulsed on and off with a pulse duration of 600 μs and a duty cycle of 50%, but the two are 90° out of phase. The output pulses from the neutral product detector are fed in parallel to two scalars gated in such a manner that the true signal is given by the difference of the two scalar readings. The phasing of the beam pulsing and the scalar gating is regularly alternated to eliminate possible spurious effects caused by irregular pulse shapes and uneven scalar gate lengths.

Even using this double beam pulsing system, however, it is still possible to have a background count rate which is indistinguishable from the true signal count rate. These spurious background effects have been described previously in some detail (Harrison, 1966a), and are generally caused by space charge interaction of the two beams giving rise to a modulated component of the background. The most effective test for the presence of such spurious signal is to observe the apparent cross-section below the threshold energy of the reaction being studied (Dolder, Harrison and Thonemann, 1961, 1963; Harrison, Dolder and Thonemann, 1963); however, the threshold for electron detachment from H^- is 0.75 eV, and it was not possible in this experiment to make observations below this threshold. Several alternative tests for spurious signal were therefore adopted.

An effective test for any spurious signals due to space charge interaction of the two beams in a crossed charged beam experiment is to measure the apparent cross-section as a function of ion beam energy keeping the incident electron energy constant. The magnitude of such spurious effects will in general depend upon the ion beam energy since the effects are basically electrostatic in nature. In order to perform this test the neutral product detector efficiency was calibrated for each ion beam energy (Section 5). The results of the test are shown in Fig.5; although the background count rate varied by about 30% over this energy range, the measured cross-section was invariant above 10 keV. At 5 keV, the apparent cross-section was 14% low, indicating the presence of spurious signal at this ion beam energy.

A further source of spurious signal may arise due to the fact that particle multipliers do not in general have a uniform detection efficiency over their surface area. It is possible that when the electron beam was pulsed on the electron space charge could alter slightly the trajectory of ions entering the collision region, thus causing the neutrals to strike the multiplier in a region of different sensitivity. This would result in a change of the background count rate when both beams were pulsed on, and the effect would be indistinguishable from true signal. In order to test for this effect, the beam separator magnet was turned off and a low-intensity beam of H^-($\sim 10^{-15}$A) was directed into the neutral product detector. The normal procedure for measuring a cross-section (Section 6) was then followed. No statistically significant signal was observed. Under these circumstances any apparent signal would have provided an upper limit on the spurious signal present in the experiment due to non-uniform multiplier sensitivity. This is because in the experiment the background of neutral particles present was formed by collisions of parent ions with residual gas both before and after the collision region, but the electron space charge could not influence the trajectories of neutral particles formed before the collision region.

If neutral particles or photons produced by the parent ion beam striking its collector can be reflected into the neutral product detector a background count rate will result which may appear partially as spurious signal due to the movement of the ion beam by the electron beam space charge. To test for the presence of such spurious signal, the cross-section with ion and electron energies fixed was measured for several values of the field of the beam separator magnet, corresponding to the parent ion beam being directed into the center of its collector, onto either edge of its collector, and completely outside its collector. The results are shown in Fig.6. No change in the cross-section was observed.

5. CALIBRATION OF NEUTRAL PRODUCT DETECTOR

In order to determine the absolute cross-section it was necessary to have accurate measurement of the efficiency of neutral particle detection. In the present experiment fast neutral particles were detected by means of a particle multiplier operated as a single particle counting device. This mode of operation has certain advantages over the more common current amplification mode. In the current amplification mode, the observed signal is directly proportional to the current gain of the multiplier, and it is difficult to keep this gain constant over reasonable periods of time. In the single particle counting mode, however, each incident neutral produces a pulse of charge, and all pulses above a minimum pulse height determined by the discriminator are counted. If the average pulse height is large compared with the discriminator level, the efficiency of detection is insensitive to the overall current gain of the multiplier, and problems of drift are greatly reduced.

It is difficult to produce an accurately known flux of energetic neutral particles for purposes of calibration, so the method adopted was to measure the detection efficiency of the multiplier for both H^- and H^+ ions, and to assume that the efficiency for H^0 was intermediate between them. This is a reasonable assumption if the detection efficiencies measured are both close to 100%.

For calibration of the neutral product detection system, a low-intensity beam of H^- or H^+ ions was allowed to enter the Faraday cup of the neutral product detector, and the current was measured with a vibrating reed electrometer. Dividing this current by the electronic charge e gives the true count rate R_T. The neutral product detector was then moved into its alternate position, in which the beam strikes the first dynode of the multiplier, and the measured count rate R_M was obtained.

In order to determine the true counting efficiency, it is necessary to take account of the dead time of the counting system. The dead time may be defined as the length of time after receiving a pulse that the counting system is incapable of registering another pulse. If the dead time is comparable with the reciprocal of the counting rate, correction must be made for pulses which are not counted. Assuming that pulses arrive randomly in time,

$$R_T = \frac{1}{\Omega} \frac{R_M}{1 - \tau R_M}$$

where τ is the dead time, and Ω is the counting efficiency. This can be expressed more conveniently as

$$\frac{1}{R_T} = \left(\frac{1}{R_M} - \tau \right) \Omega$$

For each calibration, R_T and R_M were determined for a number of different beam currents, and $1/R_T$ was plotted as a function of $1/R_M$. The counting efficiency was then determined from the slope, and the dead time from the R_M intercept. A typical plot is shown in Fig.7. In practice, the dead time of the counting system was determined by the discriminator, which was set for a value of one microsecond. The average dead time as determined from plots of $1/R_T$ versus $1/R_M$ coincided closely with this value.

The measured efficiencies of H^- and H^+ ions were always within 3% of each other, with the H^+ efficiency being slightly smaller, and both were always above 90%. The efficiency was found to drift downwards by about ½% per day when a new multiplier was put into the system, but after a few weeks no further drift was observed.

6. DETERMINATION OF THE CROSS-SECTION

For each electron beam energy, the signal count rate as a function of electron beam was measured for a number of currents from zero to a maximum value limited by the space-charge divergence of the electron beam. This divergence was monitored by measuring the current to the defining plate D (Fig.2). The current to plate D was normally a few per cent of the total electron beam current except at the lowest electron energies used, where it was allowed to rise to ten per cent. This current, corrected for loss of secondary electrons, was added to the electron collector current to give the total electron current.

Each signal measurement consisted of six 100 second counting periods. The signal normalised to ion beam current was plotted as a function of electron beam current, and the term R/IJ in equation (1) was determined from the slope of a least squares straight-line fit to this data.

The mean electron energy was calibrated absolutely to ± 0.3 eV by observing the apparent threshold for the reaction $e + Ne^+ \rightarrow Ne^{++} + 2e$ and comparing this with the spectroscopic threshold of 41.07 eV. The electron energy spread, as determined from retarding potential measurements, was about 1 eV full width at half-height.

The beam overlap factor F, which can take on values from 0 to 1, was measured at one or more electron currents for each electron energy; due to the uniformity of the ion beam current density distribution F was always greater than 0.99. The ion beam height h was measured at the same time as F.

7. RESULTS AND DISCUSSION

The results of the present experiment are shown in Fig.8. The error bars represent 90% confidence limits on the slope of R/I as a function of J. Aside from these random errors, there may be systematic errors in the measurement of the various quantities in equation (1), and there may be a systematic error due to the presence of a small undetectable amount of spurious signal. The various sources of systematic error, and the estimated maximum contribution from each source, are shown in Table 1. Table 2 presents the cross-section at each incident electron energy, and the random and maximum systematic errors associated with each measurement.

There is some indication of structure in the cross-section in the region of 30 eV, which may be due to reactions in which the product hydrogen atom is excited.

Fig.8 also shows the measurement of Tisone and Branscomb (1966) and the calculations of McDowell and Williamson (1963, 1966). The error bars on the Tisone and Branscomb measurement correspond to 50% confidence limits on the random errors; these should be multiplied by about 2½ to make them comparable with the 90% confidence limits of the present experiment. There is also a quoted systematic error on the Branscomb and Tisone measurement of +38%, -58%. Considering the quoted errors, therefore, the two experiments agree quite well.

The theory of McDowell and Williamson consists of two separate calculations which have been joined together at 40 eV. The agreement with the present experiment at electron energies above 20 eV is remarkably good; below 20 eV, however, the calculated cross-section rapidly becomes larger than the measured cross-section. Other theoretical calculations (Section 1) give results considerably different to those of the experiment.

The Born approximation predicts that for high electron energies, the functional form of the cross-section should be

$$Q = \frac{A}{E} \log \frac{E}{B}$$

However, this applies only to the cross-section before the Coulomb correction is applied. The semi-classical Coulomb correction derived by Geltman (1960) is

$$Q_c = \left(1 - \frac{2\sqrt{\pi}}{E\sqrt{Q_u}} \right) Q_u$$

where Q_c and Q_u are the corrected and uncorrected cross-sections in πa_o^2, and E is the incident electron energy in Rydbergs. In order to test the measured cross-section for the functional form predicted by the Born approximation, we must apply the Geltman correction term in reverse to the measured cross-section Q_m,

$$Q_u = \left(\frac{\sqrt{\pi}}{E} + \sqrt{\frac{\pi}{E^2} + Q_m} \right)^2$$

The magnitude of the Coulomb effect is quite significant in the energy range of the present experiment; it varies from 5% at 500 eV to 50% at 10 eV. The functional form of the experimental data with the Coulomb effect removed is displayed in Fig.9, where QE is plotted as a function of log E . The best fit to the straight line formed by the data points gives

$$Q_u = \frac{950}{E} \log \frac{E}{0.92}$$

and the functional dependence agrees well with the Born approximation prediction. From this information, a functional dependence for the cross-section with the Coulomb effect included may be derived,

$$Q_m \approx \left(1 - \frac{1.6}{\sqrt{E \log E}} \right) \frac{950}{E} \log \frac{E}{0.92} \qquad (E > 10 \text{ eV})$$

where Q_m is in units of 10^{-16} cm^2 and E is in eV.

8. ACKNOWLEDGEMENTS

We gratefully acknowledge the skilled assistance of R.R. Harrison, G.H. Hirst, and B.E. Povey in the design and manufacture of equipment, and the help of Philip Thonemann during the early part of the experiment. We are indebted to Dr P.C. Thonemann for his advice and encouragement and also to the Director of Culham Laboratory for his support of these investigations.

9. REFERENCES

BOLDT, G., 1959, Z. Phys., 154, 319, 330.
DANCE, D.F., HARRISON, M.F.A., and SMITH, A.C.H., 1966, Proc. Roy. Soc., A290, 74.
DOLDER, K.T., HARRISON, M.F.A., and THONEMANN, P.C., 1961, Proc. Roy. Soc. A264, 367.
DOLDER, K.T., HARRISON, M.F.A., and THONEMANN, P.C., 1963, Proc. Roy. Soc. A274, 546.
GELTMAN, S., 1960, Proc. Phys. Soc. 75, 67.
GELTMAN, S., 1962, Astrophys. J. 136, 935.
HARRISON, M.F.A., DOLDER, K.T., and THONEMANN, P.C., 1963, Proc. Phys. Soc. 82, 368.
HARRISON, M.F.A., 1966a, Brit. J. App. Phys. 17, 371.
HARRISON, M.F.A., 1966b, Methods of experimental physics, vol.8, to be published.
JOHN, T., 1960, Mon. Not. R. Astr. Soc. 121, 41.
McDOWELL, M.R.C., and WILLIAMSON, J.H., 1963, Phys. Letters, 4, 159.
McDOWELL, M.R.C., and WILLIAMSON, J.H., 1966, private communication.
PAGEL, B.E.J., 1956, Mon. Not. R. Astr. Soc. 116, 608.
PAGEL, B.E.J., 1959, Mon. Not. R. Astr. Soc. 119, 609.
ROGALSKI, M., 1966, Acta Phys. Polon. 29, 15.
RUDGE, M.R.H., 1964, Proc. Phys. Soc. 83, 1.
SMIRNOV, B.M., and CHIBISOV, M.I., 1966, Sov. Phys. JETP, 22, 585.
TISONE, G., and BRANSCOMB, L.M., 1966, Phys. Rev. Letters, 17, 236.

TABLE 1

POSSIBLE SOURCE OF SYSTEMATIC ERROR	MAXIMUM POSSIBLE SYSTEMATIC ERROR IN CROSS-SECTION (%)
Calibration of neutral product detector	+ 8.75, - 5.75
The measurement of I	+ 2.25, - 3.25
J	+ 0.25, - 1.25 ⁄
V	+ 0, - 0.1
v	0 ⁄
h	± 0.2
F	± 0.2
Possible spurious signal	± 2*
Uncertainty in angle of beam intersection	+ 0, - 0.5

⁄ Becomes larger at low electron energies

* Represents the limit of accuracy of the tests for spurious signal

TABLE 2

Mean incident electron energy* (eV)	Cross-section (10^{-16} cm^2)	Random error (± %)	Maximum systematic error (± %)
8.9	43.9	11	19
10.9	47.0	10	17
12.9	49.8	7	16
15.6	49.9	6	16
20.6	44.6	5	15
25.6	39.8	5	15
30.6	38.2	3	14
35.6	35.2	3	14
45.6	28.2	3	14
55.6	25.6	4	14
65.6	23.9	3	14
85.6	19.6	5	14
105.6	17.0	4	14
155.6	12.9	4	14
205.6	10.2	5	14
305.6	6.9	5	14
505.6	4.7	9	14

* ± 0.3 eV

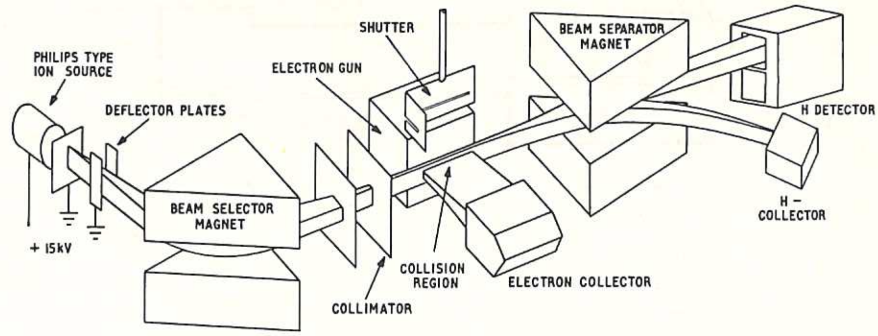

Fig. 1 Schematic view of the apparatus (CLM-P 131)

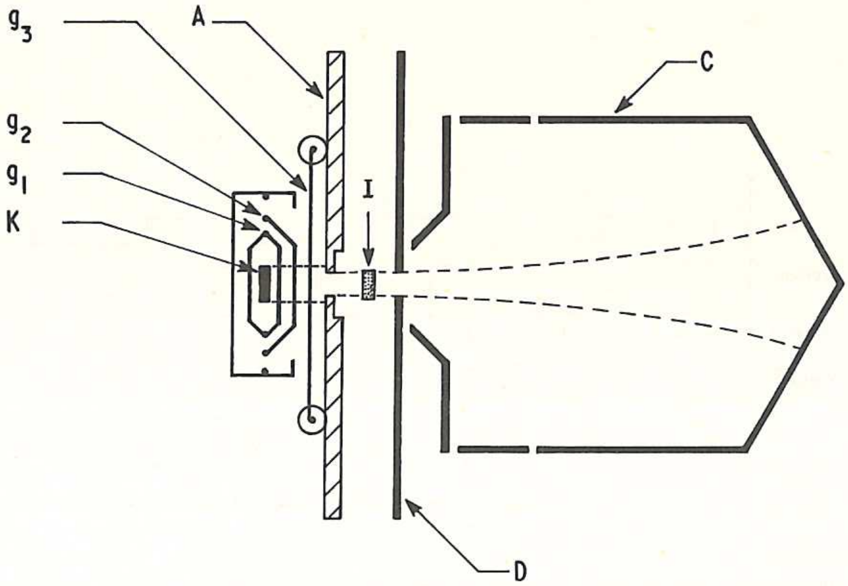

Fig. 2 (CLM-P 131)

View of the apparatus through the electron beam. K, cathode; g_1, control grid; g_2, accelerating grid; g_3, suppressor grid; A, anode; I, ion beam; D, defining plate; C, collector. g_2 and g_3 were always biased positive with respect to A, so that secondary electrons formed at g_2, g_3, and A could not enter the collision region

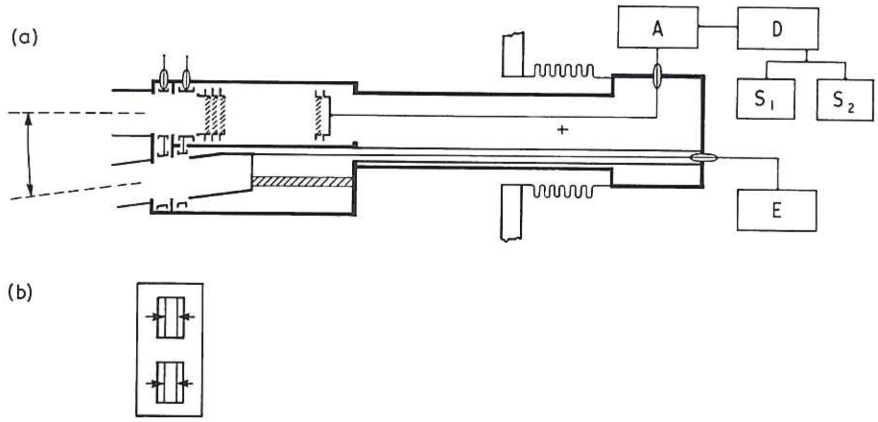

Fig. 3 (CLM-P 131)

(a) Sectional view of neutral product detector. A, pulse amplifier; D, discriminator; S1, S2, scalers; E, vibrating reed electrometer. This detector contains both a particle multiplier and a Faraday cup, and is moveable so that either may intercept the incident beam

(b) Front view of neutral product detector, showing variable entrance apertures

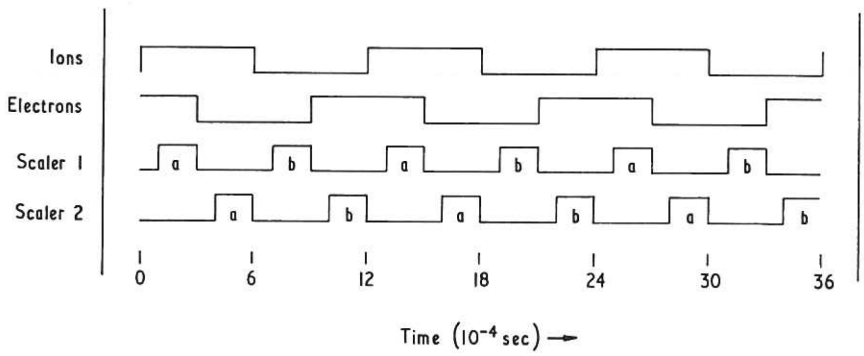

Fig. 4 (CLM-P 131)

Waveforms of ion and electron beams, and scaler gates. If B_i and B_e are the backgrounds produced by the ion and electron beams, B_d is the background due to electronic noise, and R is the signal, then scaler 1 measures $[R + B_i + B_e + B_d]a + [B_d]b$ and scaler 2 measures $[B_i + B_d]a + [B_e + B_d]b$ where the subscripts outside the brackets refer to the appropriate counting periods. The difference in the scaler readings gives the signal R

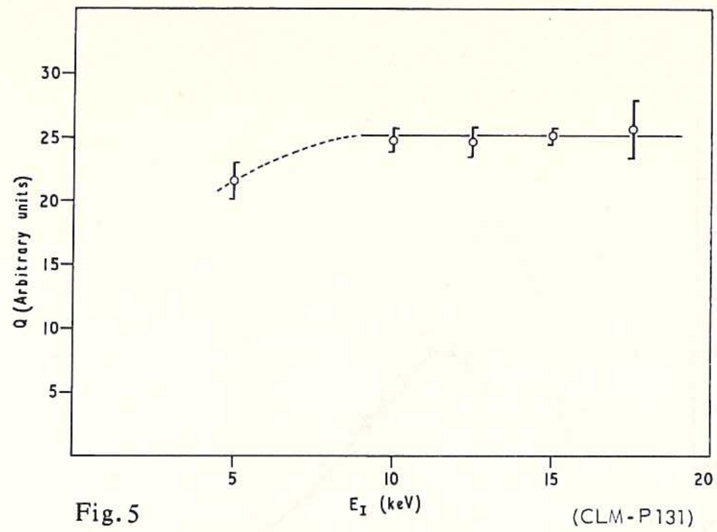

Fig. 5 (CLM-P 131)
Variation of measured cross-section with ion beam energy at an incident electron energy of 50 eV. Brackets indicate 90% confidence limits

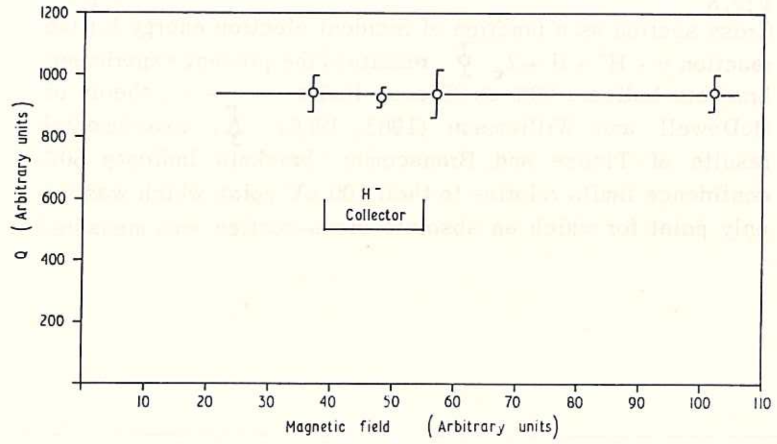

Fig. 6 (CLM-P 131)
Variation of measured cross-section with magnetic field of beam separator magnet at an incident electron energy of 50 eV. Brackets indicate 90% confidence limits

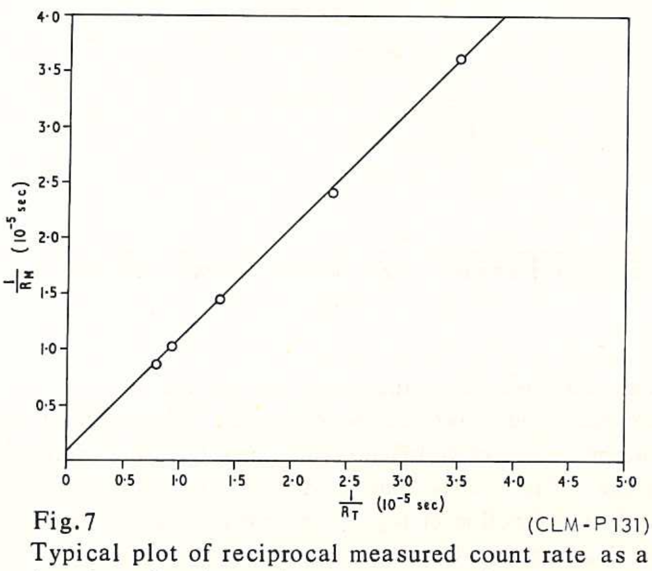

Fig. 7 (CLM-P 131)
Typical plot of reciprocal measured count rate as a function of reciprocal true count rate for the neutral product detector. From this plot the counting efficiency and the dead time can be determined (see text)

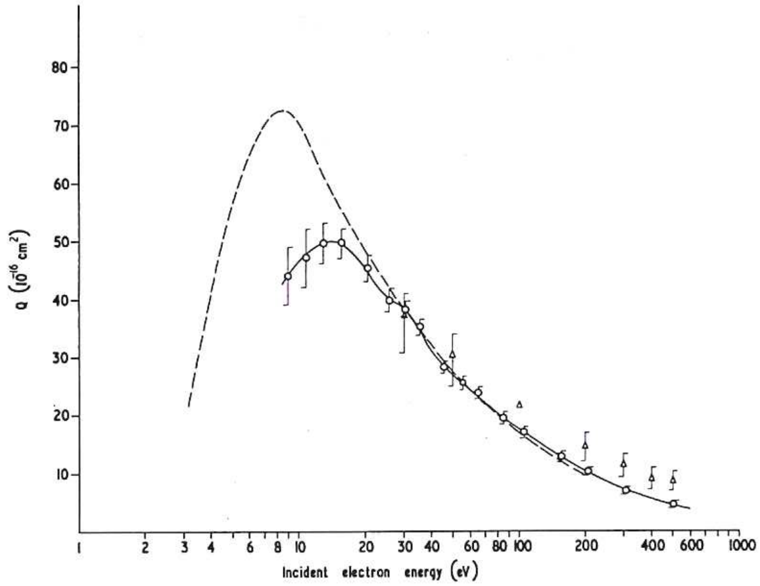

Fig. 8 (CLM-P131)
Cross section as a function of incident electron energy for the reaction $e + H^- \rightarrow H + 2e$ ⟟, results of the present experiment; brackets indicate 90% confidence limits. - - - - , theory of McDowell and Williamson (1963, 1966). ⟟, experimental results of Tisone and Branscomb; brackets indicate 50% confidence limits relative to their 100 eV point, which was the only point for which an absolute cross-section was measured

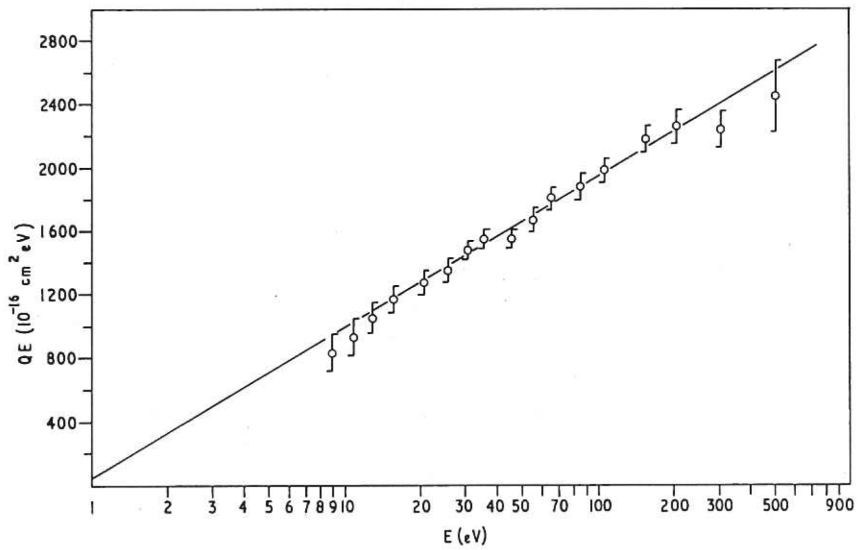

Fig. 9 (CLM-P131)
Functional dependence of the cross-section for $e + H^- \rightarrow H + 2e$. Q is the measured cross-section with the Coulomb effect removed using the procedure of Geltman (1960), and E is the incident electron energy. The results show a straight line behaviour when QE is plotted as a function of log E, indicating that the cross-section with the Coulomb effect removed is a function of log E/E